Supporting Information Table S1.

X-ray data collection and refinement statistics

Data Collection	
Space group	*C222₁*
Cell Dimensions *a, b, c* (Å)	*a = 73.2, b = 92.3, c = 165.7*
Wavelength (Å)	1.5418
Resolution Range (Å)	50.00 - 2.26 (2.34 - 2.26)
R_{merge}	0.062 (0.182)
I/σ(I)	38.6 (13.1)
Completeness (%)	95.2 (90.5)
Redundancy	9.4 (9.2)
No. of copies / a.s.u.	3
Temperature	100 K
Refinement	
Resolution (Å)	82.76 – 2.26 (2.32 - 2.26)
No. reflections R_{work}	24020 (1639)
No. reflections R_{free}	1299 (81)
R_{work}	0.17 (0.16)
R_{free}	0.23 (0.29)
No. atoms	
Protein	3515
Peptide	376
Solvent	334
R.m.s. deviations	
Bond lengths(Å)	0.015
Bond angles (°)	1.6
Chiral ($Å^3$)	0.115

Values in parentheses represent statistics for highest resolution shell.

Diffraction data were collected from the frozen crystal at 100K with a Raxis 4++ image plate detector mounted on a Rigaku Micromax 007 rotating anode X-ray generator equipped with an AXCO capillary optic (CuKa radiation λ = 1.54 Å). The diffraction data were processed with HKL2000.[1] The structure was obtained by molecular replacement with PHASER[2] using the structure of Bcl-x_L from the $Beclin^{BH3}$/Bcl-x_L complex (PDB ID: 2P1L) as a search model. The final model was built following several rounds of building and refinement using Coot[3] and Refmac5.[4]

[1] Z. Otwinowski, W. Minor, *Macromolecular Crystallography, Pt. A Methods in Enzymology* **1997**, *276*, 307.

[2] L. C. Storoni, A. J. McCoy, R. J. Read, *Acta Crystallogr D Biol Crystallogr* **2004**, *60*, 432.

[3] P. Emsley, K. Cowtan, *Acta Crystallogr D Biol Crystallogr* **2004**, *60*, 2126.

[4] G. N. Murshudov, A. A. Vagin, E. J. Dodson, *Acta Crystallogr D Biol Crystallogr* **1997**, *53*, 240.

Supporting Information Figure S1. Three molecules are present in the asymmetric unit. **a)** Molecules A and B are related by a non-crystallographic dyad symmetry axis and form a domain swapped dimer similar to that reported previously.[15b] **b)** Molecule C engages a crystallographic dyad symmetry axis to also form a domain swapped dimer. The dimer interface in this case is different to that seen previously, but in both cases the BH3-binding groove is remote from and unaffected by the dimer interface.

Supporting Information Figure S2. Overlay of the backbone trace of Bcl-x_L in complex with Bim^{BH3} (blue) and the foldamer of molecules A (green), B (pink) and C (yellow). The orientation of the figure is as in Figure 2 and the peptide ligands have been removed. Note the variability in the conformation of helix α3 on the right hand side of the binding groove. In all three molecules of Bcl-x_L in complex with the foldamer, Leu108 occludes the *h1* pocket, whilst in the Bim^{BH3}/Bcl-x_L complex Leu108 is in a different orientation accommodating Ile58 of Bim^{BH3}.

Supporting Information Figure S3. Direct-binding fluorescence polarization binding assay data showing interaction of wild-type Bcl-x_L (closed circles) or the Bcl-x_L A142L mutant (open circles) with fluorescein-labeled ligands: **a) Flu-Bak^{BH3}** (Flu-GQVGRQLAIIGDDINR-NH_2), **b) Flu-Bad^{BH3}** (H_2N-NLWAAQRYGRELRRMSDK*FVDSFKK-NH_2; K* = lysine, labeled on the side chain with fluorescein), and **c) Flu-Ahx-2** (Flu-Ahx-APC-Ala-ACPC-Arg-ACPC-Leu-ACPC-Lys-β^3hNle-Gly-Asp-Ala-Phe-Asn-Arg-NH_2; Ahx = aminohexanoic acid).

Supplementary Figure S1

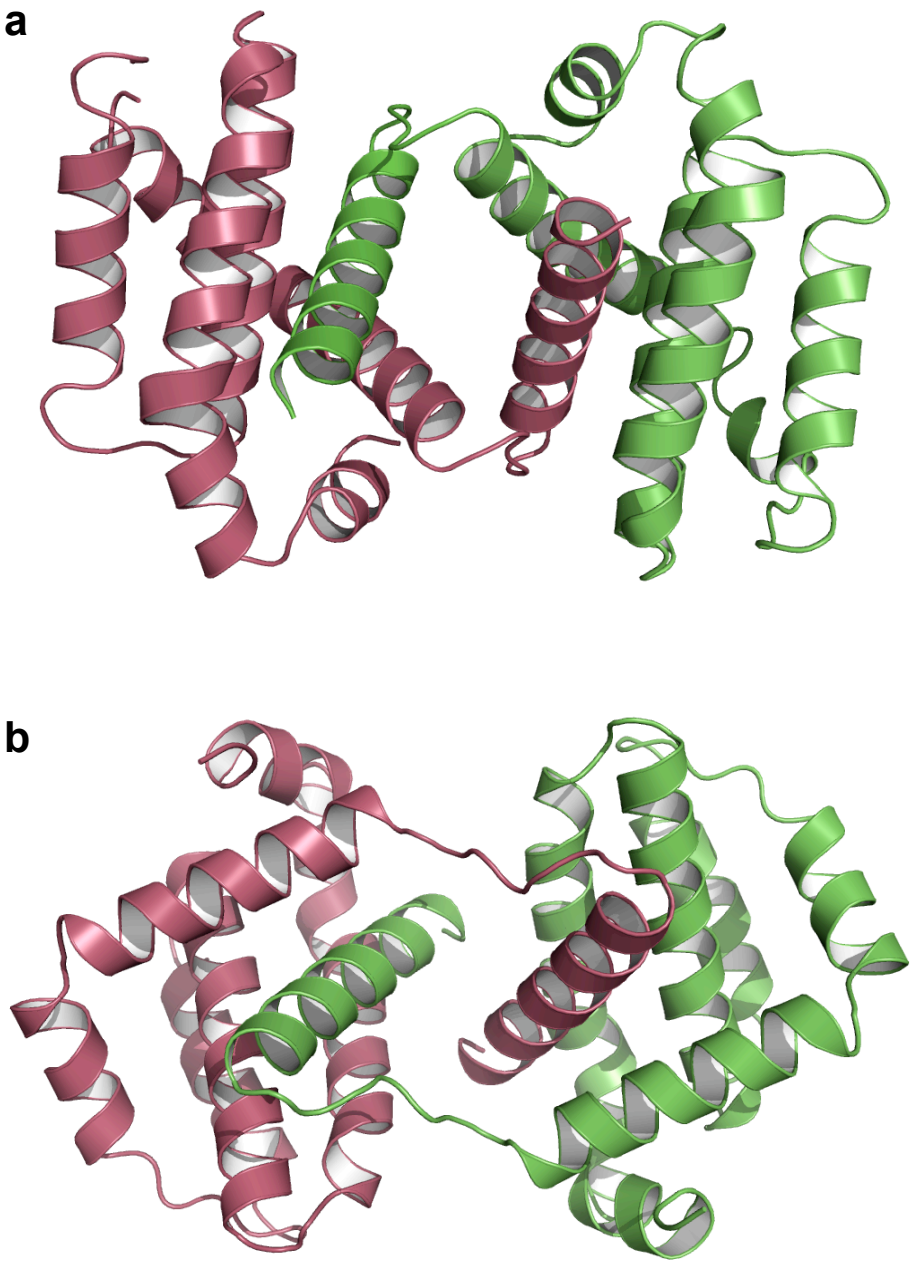

Supplementary Figure S2

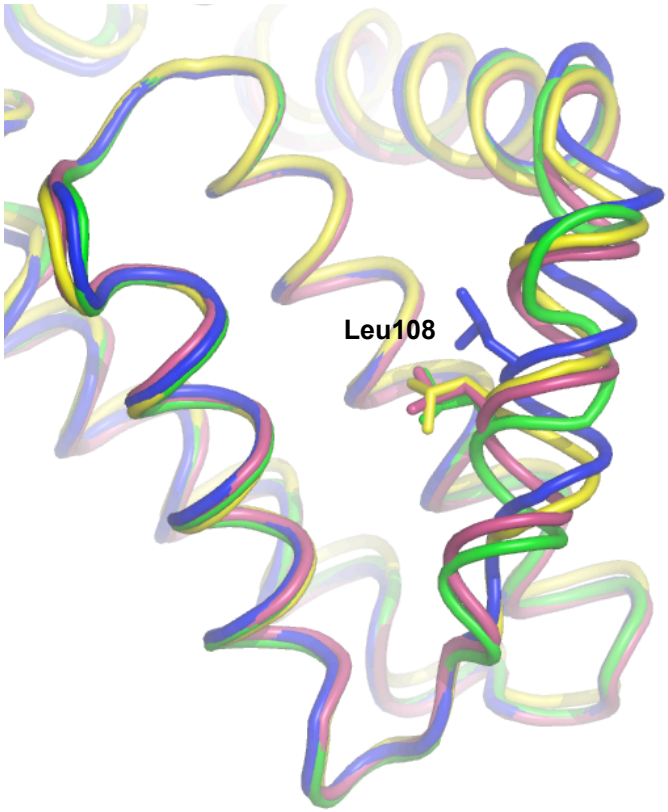

Supplementary Figure S3

a (Flu-Bak^{BH3})

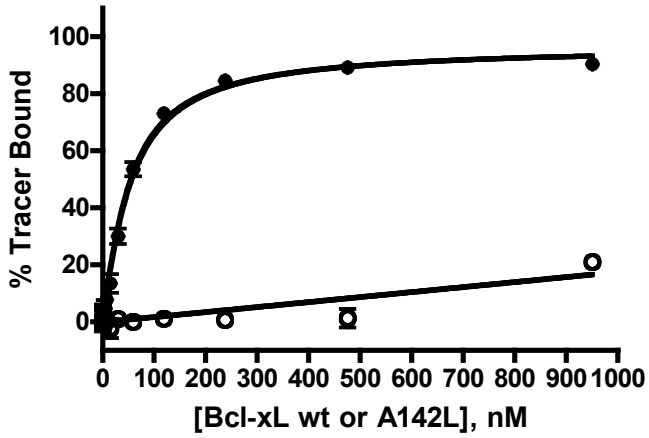

b (Flu-Bad^{BH3})

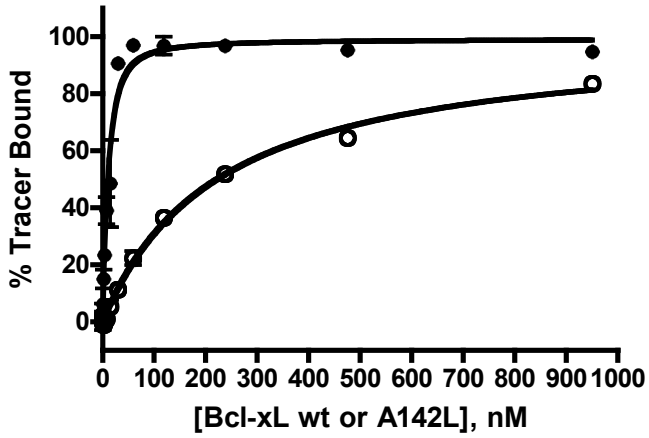

c (Flu-Ahx-**2**)